

Geomaterials (Petrology)
**Chromitite potential in mantle peridotites of the
Jandaq ophiolite (central Iran)**

Ghodrat Torabi

Department of Geology, University of Isfahan, Azadi Square, 8174673441 Isfahan, Iran

Received 13 June 2008; accepted after revision 27 July 2009

Available online 14 October 2009

Presented by Jacques Angelier

Abstract

Mantle peridotite (Iherzolite) is one of the most important rock units of the Jandaq ophiolite (central Iran). This ophiolite suffered numerous phases of metamorphism, and is covered by Paleozoic schist and marble metamorphic rocks. Metamorphic minerals found are olivine, tremolite, orthopyroxene, talc, anthophyllite, chlorite, serpentine and magnetite. Clinopyroxene and chromian spinel, the most resistant minerals against metamorphism and alteration, are relicts of the primary igneous mineralogy. One of the most important characteristics of the mantle peridotites in Jandaq ophiolites is the absence of chromitite, due to the low Cr- and high Al-nature of these mantle rocks, as well as non-extensive mantle partial melting during continual production of ascending melt. The Jandaq peridotite belongs to the LOT-type, and has no chromitite potential. **To cite this article: G. Torabi, C. R. Geoscience 341 (2009).**

© 2009 Académie des sciences. Published by Elsevier Masson SAS. All rights reserved.

Résumé

Les péridotites de l'ophiolite de Jandaq (Iran central) peuvent-elles renfermer des gisements de chromite ? Une péridotite mantellique Iherzolitique est l'un des types pétrographiques principaux constituant l'ophiolite de Jandaq (Iran central). Recouverte de marbres et schistes paléozoïques, cette ophiolite a subi de nombreuses phases de métamorphisme. Les minéraux métamorphiques sont olivine, trémolite, orthopyroxène, talc, antophyllite, chlorite, serpentine et magnétite. Clinopyroxène et spinelle chromifère, plus résistants au métamorphisme et à l'altération, sont des reliques de la minéralogie ignée primaire. L'une des caractéristiques les plus importantes de l'ophiolite de Jandaq est l'absence de chromitites, liée au caractère pauvre en chrome et riche en aluminium de ces roches mantelliques, ainsi qu'à la fusion partielle limitée du manteau durant une production continue de laves ascendantes. De type LOT, la péridotite de Jandaq n'a ainsi aucun potentiel chromifère. **Pour citer cet article : G. Torabi, C. R. Geoscience 341 (2009).**

© 2009 Académie des sciences. Publié par Elsevier Masson SAS. Tous droits réservés.

Keywords: Chromitite; Ophiolite; Mantle peridotite; Jandaq; Central Iran

Mots clés : Chromitite ; Ophiolite ; Péridotite mantellique ; Jandaq ; Iran central

E-mail address: torabighodrat@yahoo.com.

1. Introduction

1.1. Geological background

Chromitite, a rock chiefly containing the chromite mineral, is the major source of chromium and a common rock-type in many ophiolite massifs. The mechanism of chromian spinel concentration in podiform chromitites has been discussed in many papers (e.g. [4,5,19,24,27,34]), but it has not yet been completely solved. Chromitites are able to record petrogenetic processes in the upper mantle. However, the study of many ophiolites reveals that they are not equally distributed among a mantle section of ophiolite complexes. In some cases, chromitites are never observed, contrasting with the majority of ophiolites in which chromitite is present in the transition zone [8,22,23]. This important observation has been elaborated in 1985 by F. Boudier and A. Nicolas, with the LOT-and HOT- ophiolite types [8], see also [19,23,24]. Chromitite is generally absent in ophiolites that are characterized by a lherzolite-dominant mantle section (Lherzolite Ophiolite Type [LOT]). On the contrary, it is present in ophiolites where this section is harzburgitic (Harzburgite Ophiolite Type [HOT]).

As the initial source of chromium is contained in clinopyroxene (diopside) [8], the degree of partial melting plays an essential role for the eventual formation of chromitites. In LOT-peridotites, which have suffered a low-degree of partial melting, chromium hosted by clinopyroxene is still largely retained in this mineral. In HOT-systems, on the other hand, the clinopyroxene of fertile mantle peridotite has been molten. As a result, chromium has been incorporated into the basaltic melt. This increases the possibility for the later segregation of chromium into chromitites during basalt crystallization [24].

Petrography of mantle peridotites of the Jandaq ophiolite shows that this ophiolite is of the LOT type, and based on the general trend, it should not contain the chromitite. Despite the general rule, some LOT ophiolites have chromitite (e.g. [8,15,24]), and paucity of chromite mineralization in some HOT is presented (e.g. [33]). These exceptions show the necessity of chromitite potential study on the Jandaq ophiolite as one of the important Iranian ophiolites.

Chromitites are present in most of Iranian ophiolites (e.g. Neyriz, Naein, Esfandagheh, Sabzevar, Faryab and Ashin), all belonging to the HOT-type [30,32]. However, they have not been found in other occurrences (e.g. Anarak, Posht-e-Badam and Jandaq, Bayazeh), which until now have not been studied in great detail.

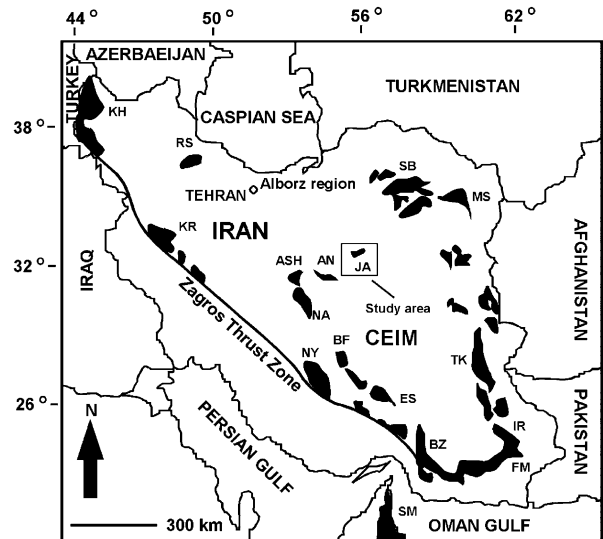


Fig. 1. Main ophiolites of Iran and location of the Jandaq ophiolite. KH: Khoy; KR: Kermanshah; NY: Neyriz; BZ: Band Ziarat; NA: Naein; BF: Baft; ES: Esfandagheh; FM: Fanuj-Maskutan; IR: Rasht; TK: Tchehel Kureh; MS: Mashhad; SB: Sabzevar; RS: Rasht; SM: Samail; ASH: Ashin; AN: Anarak; JA: Jandaq.

Fig. 1. Principales ophiolites d'Iran, emplacement de l'ophiolite de Jandaq. KH: Khoy; KR: Kermanshah; NY: Neyriz; BZ: Band Ziarat; NA: Naein; BF: Baft; ES: Esfandagheh; FM: Fanuj-Maskutan; IR: Rasht; TK: Tchehel Kureh; MS: Mashhad; SB: Sabzevar; RS: Rasht; SM: Samail; ASH: Ashin; AN: Anarak; JA: Jandaq.

The main aim of this paper is to check the chromitite potential of mantle peridotites in Jandaq ophiolite. This ophiolite presents good exposures of mantle peridotites in northwestern part of the Central-East Iranian Microplate (CEIM). This occurrence will then be compared with the Ashin ophiolite (Central Iran) which is a HOT with considerable amount of chromite deposits (Fig. 1). It is hoped that the comparison of Jandaq chromitite absent LOT with Ashin chromitite bearing HOT, will be useful to evaluate the chromitite potential in Jandaq ophiolite.

1.2. Geological setting

Ophiolite complexes of Iran are part of Middle East Tethyan ophiolite belts. They link to other Asian ophiolites, such as Pakistan in the east, or ophiolites in the Mediterranean region, such as Turkish, Troodos, and East Europe in the west [32]. These ophiolites rest as giant thrust sheets upon a continental substrate [23].

Iranian ophiolites (Fig. 1) have geographically been divided into four groups:

- (1) ophiolites of northern Iran along the Alborz mountain range including Rasht ophiolites;

- (2) ophiolites of Zagros suture zone including the Neyriz and Kermanshah ophiolites which are apparently the extension of the Oman ophiolites;
- (3) ophiolites and color *mélanges* of the Makran region, located in the South-East of Iran and;
- (4) ophiolites and color *mélanges* that mark the boundaries of the CEIM.

The ages of emplacement derived from field relationships suggest another three-fold classification [1]:

- (1) Proterozoic ophiolites, that crop out on the western edge of the Lut block in central Iran;
- (2) Pre-Jurassic ophiolites that are located within the Alborz range in the northern Iran and;
- (3) Post-Jurassic ophiolites that are the most abundant ophiolite terrains in Iran.

Most recent time of emplacement is not known, but suggested by Lippard et al. [22] to be pre-Paleocene.

The study area (Jandaq ophiolite) is located on the West of central Iran, and the southern margin of Great Kavir with highly deserted geographical conditions (Fig. 2), considered to be Upper Proterozoic [1,3,28] or Paleozoic [10,11]. The Jandaq ophiolite is a remnant of Paleo-Tethys, transferred to central Iran by anti-clockwise rotation of Central-East Iranian microcontinent (CEIM) [6,10,11]. The ophiolite massif is

composed of mantle peridotite and serpentized mantle peridotite, metagabbro, basic and ultrabasic metamorphosed dikes, metapyroxenite, amphibolite, rodingite, and listwaenite [31]. It has been covered by Paleozoic metamorphic rocks (schist and marble) (Fig. 2). Chromitite has not been found yet. Mesozoic granite and mylonitic granite intrusions crosscut the Jandaq ophiolite and the covering metamorphic rocks. Chah-palang formation with Upper Jurassic age, and lithology of sandstone, siltstone and conglomerate, together with the Cretaceous limestone, have been covered by the Jandaq ophiolite, metamorphic rocks and granitic intrusions (Fig. 3A).

All rock units of the Jandaq ophiolite have been highly metamorphosed, and they have suffered a high degree of serpentization. Based on amphibolite suites [31], prograde metamorphism has reached upper amphibolite facies conditions (7.98–9.01 kbar and 714–737 °C). Several phases of metamorphism have certainly occurred, not deciphered in detail at present. Middle-Jurassic metamorphism is however indicated by new ^{40}Ar - ^{39}Ar isotopic analyses [6] on samples from the northern slope of Rashid Kuh, one on muscovite in micaschist (163.86 ± 1.76 Ma plateau age), the second one on hornblende in amphibolite (156.56 ± 33.15 Ma plateau age).

For detailed study of the Jandaq ophiolite, 250 rock samples were collected from all rock units of the area, during 23 days of the field study.

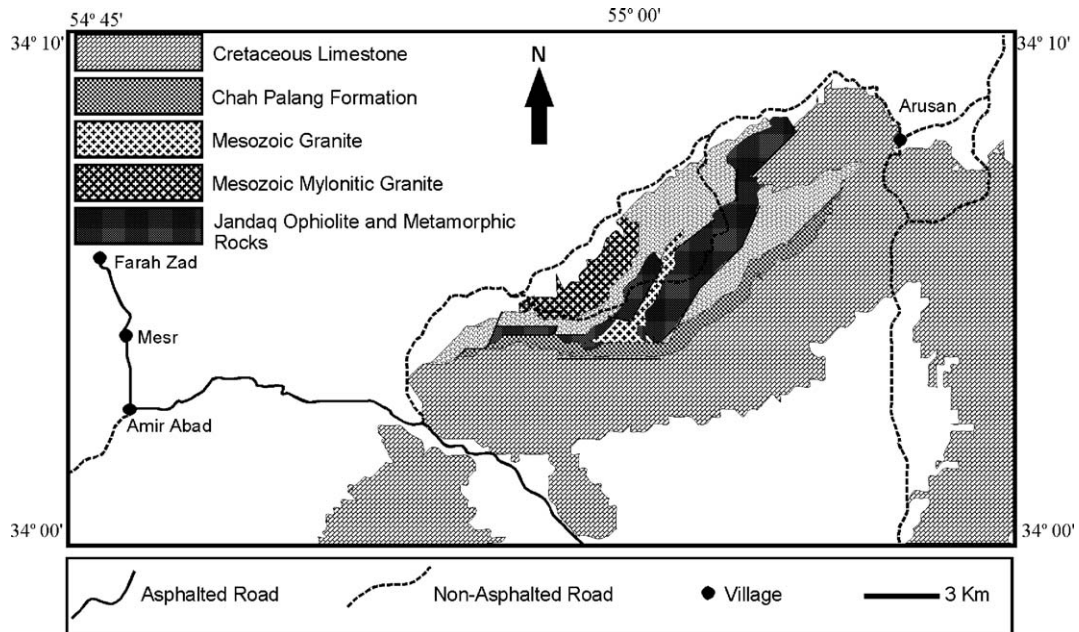


Fig. 2. Simplified geological map of the study area.

Fig. 2. Carte géologique simplifiée de la région étudiée.

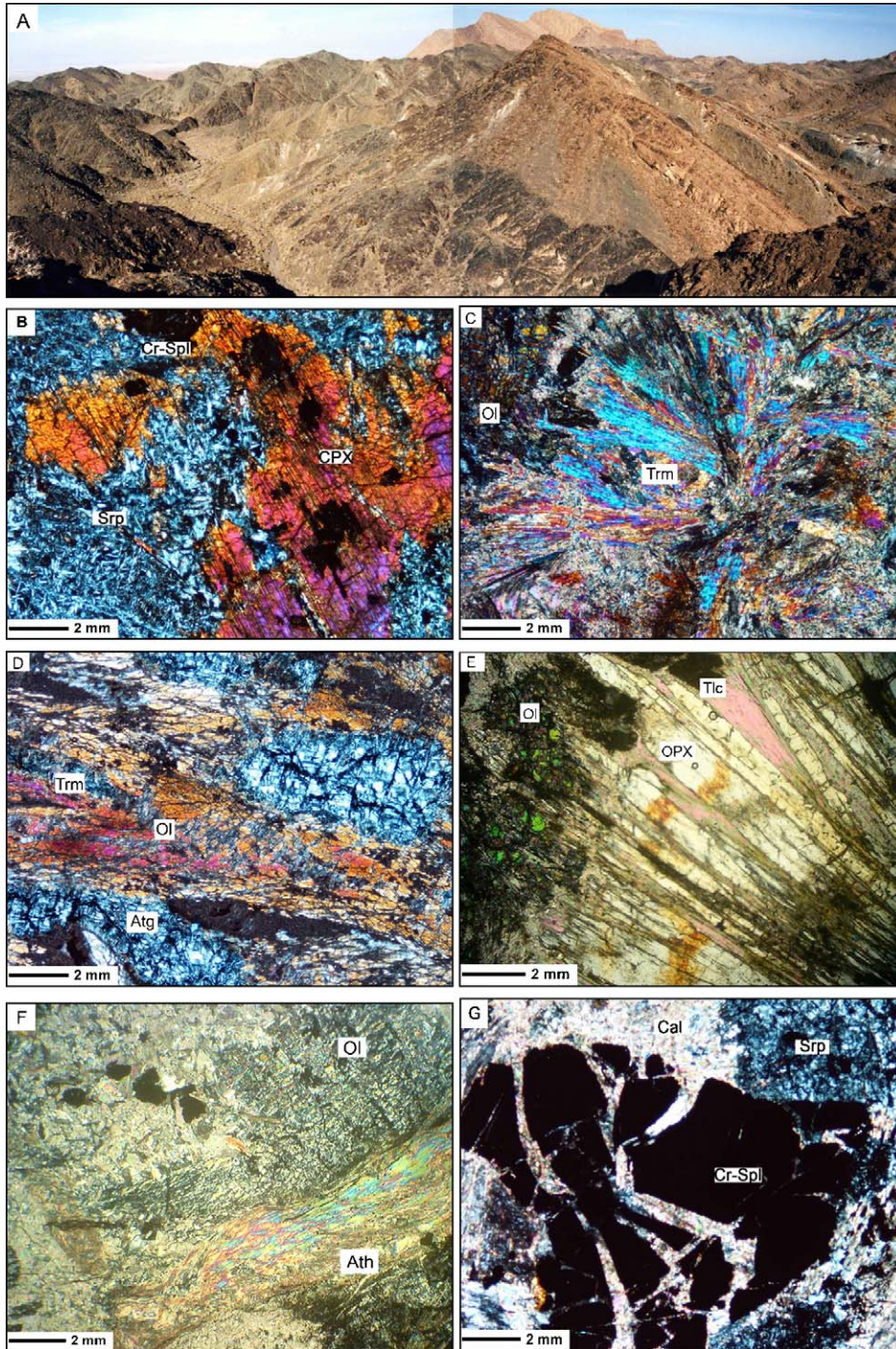


Fig. 3. Field photograph and microscopic photomicrographs of the Jandaq ophiolite mantle peridotites. (A) General view of the Jandaq ophiolite. Mantle peridotites are in the foreground, and Chahpalang formation and Cretaceous limestones are in the background. (B) Relict of igneous clinopyroxene in a lherzolite. (C and D) Photographs of tremolite-bearing metalherzolites. (E and F) Metaharzburgites with metamorphic olivine, orthopyroxene, talc and anthophyllite. (G) Relict of an igneous spinel.

Fig. 3. Affleurement et microphotographies des péridotites mantelliques de l'ophiolite de Jandaq. (A) Vue générale du massif ophiolitique. Les péridotites sont au premier-plan, la formation de Chahpalang et les calcaires crétacés en arrière-plan. (B) Relique de clinopyroxène igné dans une lherzolite. (C et D) Microphotographies de métalherzolites à tremolite. (E et F) Méta-harzburgite contenant olivine et orthopyroxène métamorphiques, talc et antophyllite. (G) Relique de spinelle magmatique.

2. Analytical data

Analysis of minerals was carried out with a Cameca SX-100 electron-probe micro-analyzer (WDS) at the Institute of Mineralogy, Leibniz University, Hanover, Germany. The analyses were performed under an accelerating voltage of 15 kV and a beam current of 15 nA with 3- μ m probe beam diameter. Natural and synthetic minerals of known composition are used as standards. The Fe⁺³ and Fe⁺² amounts of spinel were calculated assuming spinel (AB₂O₄) stoichiometry [13]. The Cr#, Mg# and Fe³⁺# are Cr/(Cr + Al), Mg/(Mg + Fe⁺²) and Fe³⁺/(Cr + Al + Fe³⁺) atomic ratio of minerals, respectively. Representative analyses of the minerals and calculated structural formulas are shown in Table 1. Mineral abbreviations in photomicrographs are from Kretz [18].

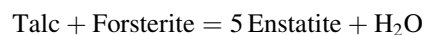
The major and trace element analyses were carried out on whole rocks at the Central laboratory of University of Isfahan by Bruker S4 Pioneer XRF, and Activation Laboratory of Isfahan (MNSR Department), by NAA method. Forty-four samples of mantle peridotites from the Jandaq and Ashin ophiolite were selected for analyses. Whole rock geochemical data are presented in Table 2.

The serpentine mineral was identified at the Central laboratory of the University of Isfahan as antigorite on the basis of its X-ray diffraction pattern by Bruker D8 Advance XRD machine.

3. Petrography and mineral chemistry

In outcrop, these metamorphosed ultramafic bodies are grayish-green to dark-green. Generally, they are extensively serpentinized, metamorphosed and sheared, retaining very little primary relict texture. Main textures of the investigated rocks are porphyroblastic, granoblastic, nematoblastic, poikiloblastic and mesh texture. The textural relationships of mantle peridotites in Jandaq ophiolite demonstrate a prograde metamorphism from partially serpentinized peridotite to metaperidotite in response to a regional metamorphism in upper amphibolite facies conditions. A retrograde metamorphism has been developed after the progression. Therefore, the studied rocks have undergone three main stages of recrystallization. An initial retrograde hydration was followed by a progressive dehydration and a final retrograde hydration. The evidence of this complex hydration and dehydration reactions is presented by minerals description:

- Clinopyroxenes (diopside with Mg# 0.91–0.97) and chromian spinels (Cr# 0.46–0.61) are relicts of the primary igneous mineralogy and are the most resistant minerals against the metamorphism and alteration. Inner part of spinels and most of clinopyroxenes are intact (Fig. 3B and 3G). The modal abundance of clinopyroxene in some rock samples reaches to 30% (very high) which partly are changed to tremolite during the metamorphism. Spinels altered to chromian magnetite in margin and their modal abundance in all samples is less than 3%. Cr₂O₃ contents of clinopyroxenes ranges from 0.71–1.31 wt% (Table 1).
- Olivines (Fo₈₈–Fo₉₂) are metamorphic, produced during progressive metamorphism. This is suggested by very irregular grain boundary relations of olivines with other metamorphic minerals and fine magnetite inclusions [26]. Olivine grains show alteration to serpentine that is one of the evidences of last hydration. Concentrations of minor elements as TiO₂, Al₂O₃ and CaO are very low. MnO content ranges up to 0.14 wt.%.
- Orthopyroxenes (enstatite with Mg# 0.89–0.96) are elongate and much coarser-grained than coexisting olivines. The margins of all orthopyroxenes are replaced by serpentine. This texture indicates that the orthopyroxene retrograde serpentinization has occurred. Al₂O₃ and Cr₂O₃ contents of analyzed orthopyroxenes are 0.49–1.94, and 0.03–0.40 wt.%, respectively. Concentrations of minor elements are low. Compositionally, the studied orthopyroxenes are similar to the reported metamorphic orthopyroxenes from other ultramafic metamorphosed rocks [14]. Orthopyroxenes occur as granoblasts to bladed grains with scalloped borders in contact with olivine and interpreted to record the prograde reaction (Fig. 3E):



- Tremolite (Mg# 0.89–1) is common in these ultramafic bodies and present prismatic crystals and some times jack-straw texture (Fig. 3C and D). Some tremolites are poikiloblastic, having inclusions of opaque minerals and chlorite that are common around igneous clinopyroxene relicts; others present intergrowth with olivine and serpentine. Tremolites and clinopyroxenes are present as the most important Ca-bearing silicates in most of these rocks. Main chemical characteristics of analyzed tremolites are low concentration of Na₂O (< 0.45% wt.%) and Al₂O₃ (< 1.62 wt.%), and high Mg# (> 0.89).
- Anthophyllite (Fe³⁺# 0.52–0.53) is magnesian amphibole of these metamorphosed peridotites and is much

Table 1

Representative chemical analyses of minerals in mantle peridotites of the Jandaq ophiolite (central Iran) and their calculated structural formula.

Tableau 1

Analyses chimiques représentatives et formules structurales calculées des minéraux des péridotites mantelliques de l'ophiolite de Jandaq (Iran central).

| Sample | CPX | CPX | Spinel | Spinel | Olivine | Olivine | OPX | OPX | Tremolite | Tremolite | Anthoph. | Anthoph. | Talc | Talc | Chlorite | Chlorite | Serpentine | Serpentine |
|--------------------------------|--------|-------|--------|--------|---------|---------|--------|--------|-----------|-----------|----------|----------|--------|--------|----------|----------|------------|------------|
| SiO ₂ | 52.42 | 52.92 | 0.00 | 0.25 | 40.72 | 41.29 | 57.43 | 57.31 | 58.34 | 57.80 | 55.62 | 56.99 | 59.91 | 61.74 | 34.48 | 33.74 | 42.28 | 43.38 |
| TiO ₂ | 0.35 | 0.27 | 0.00 | 0.41 | 0.00 | 0.01 | 0.00 | 0.04 | 0.00 | 0.00 | 0.01 | 0.01 | 0.01 | 0.00 | 0.02 | 0.03 | 0.01 | 0.02 |
| Al ₂ O ₃ | 2.34 | 5.06 | 19.75 | 28.70 | 0.00 | 0.03 | 1.08 | 0.94 | 0.31 | 0.08 | 1.60 | 1.59 | 1.14 | 0.74 | 13.11 | 13.84 | 1.69 | 1.39 |
| Cr ₂ O ₃ | 0.71 | 0.84 | 45.35 | 35.68 | — | — | 0.40 | 0.05 | 0.08 | 0.06 | 0.32 | 0.43 | 0.17 | 0.09 | 0.30 | 0.12 | 0.59 | 0.30 |
| FeO [*] | 3.46 | 2.16 | 23.16 | 19.78 | 10.88 | 7.60 | 7.05 | 5.95 | 2.31 | 3.66 | 2.90 | 2.82 | 1.40 | 1.31 | 6.50 | 6.62 | 1.92 | 1.86 |
| MnO | 0.17 | 0.08 | 0.21 | 0.77 | 0.10 | 0.07 | 0.12 | 0.15 | 0.03 | 0.05 | 0.00 | 0.00 | 0.08 | 0.03 | 0.09 | 0.10 | 0.06 | 0.05 |
| MgO | 17.07 | 15.83 | 9.17 | 12.94 | 48.64 | 51.38 | 34.25 | 35.91 | 23.83 | 22.64 | 32.99 | 34.16 | 30.53 | 30.53 | 32.47 | 32.56 | 38.74 | 39.25 |
| CaO | 23.22 | 21.68 | 0.01 | 0.04 | 0.00 | 0.00 | 0.08 | 0.09 | 13.26 | 13.60 | 0.00 | 0.04 | 0.02 | 0.03 | 0.06 | 0.02 | 0.02 | 0.00 |
| Na ₂ O | 0.33 | 0.82 | 0.02 | 0.07 | 0.01 | 0.01 | 0.02 | 0.00 | 0.07 | 0.05 | 0.01 | 0.03 | 0.46 | 0.31 | 0.02 | 0.02 | 0.00 | 0.00 |
| K ₂ O | 0.01 | 0.03 | 0.01 | 0.00 | 0.01 | 0.00 | 0.00 | 0.00 | 0.02 | 0.02 | 0.03 | 0.03 | 0.01 | 0.01 | 0.03 | 0.01 | 0.00 | 0.00 |
| NiO | 0.00 | 0.05 | 0.00 | 0.21 | 0.00 | 0.00 | 0.00 | 0.04 | — | — | — | — | — | — | — | — | 0.07 | 0.08 |
| Total | 100.08 | 99.75 | 97.68 | 98.57 | 100.36 | 100.39 | 100.43 | 100.48 | 98.17 | 97.90 | 93.16 | 95.67 | 93.56 | 94.70 | 87.08 | 87.06 | 85.38 | 86.32 |
| Oxygens # | 6 | 6 | 32 | 32 | 4 | 4 | 6 | 6 | 23 | 23 | 23 | 23 | 21 | 21 | 28 | 28 | 7 | 7 |
| Si | 1.906 | 1.922 | 0.000 | 0.061 | 0.998 | 0.997 | 1.977 | 1.955 | 7.880 | 7.927 | 6.611 | 6.586 | 7.699 | 7.866 | 6.577 | 6.452 | 2.013 | 2.033 |
| Ti | 0.010 | 0.007 | 0.000 | 0.075 | 0.000 | 0.001 | 0.000 | 0.001 | 0.000 | 0.000 | 0.001 | 0.001 | 0.001 | 0.000 | 0.003 | 0.004 | 0.000 | 0.001 |
| Al | 0.10 | 0.217 | 6.061 | 8.190 | 0.000 | 0.000 | 0.044 | 0.038 | 0.049 | 0.013 | 0.224 | 0.216 | 0.173 | 0.111 | 2.952 | 3.121 | 0.095 | 0.077 |
| Cr | 0.020 | 0.024 | 9.333 | 6.830 | — | — | 0.011 | 0.001 | 0.009 | 0.006 | 0.030 | 0.039 | 0.003 | 0.001 | 0.045 | 0.018 | 0.020 | 0.011 |
| Fe ²⁺ | 0.033 | 0.066 | 4.448 | 3.296 | 0.223 | 0.153 | 0.203 | 0.121 | 0.000 | 0.306 | 0.000 | 0.000 | 0.150 | 0.140 | 0.954 | 1.034 | 0.076 | 0.073 |
| Fe ³⁺ | 0.072 | 0.000 | 0.600 | 0.709 | 0.00 | 0.00 | 0.000 | 0.048 | 0.261 | 0.115 | 0.288 | 0.273 | 0.000 | 0.000 | 0.082 | 0.025 | 0.000 | 0.000 |
| Mn | 0.005 | 0.003 | 0.006 | 0.158 | 0.002 | 0.001 | 0.003 | 0.004 | 0.003 | 0.006 | 0.000 | 0.000 | 0.009 | 0.003 | 0.015 | 0.016 | 0.002 | 0.002 |
| Mg | 0.925 | 0.857 | 3.558 | 4.671 | 1.778 | 1.849 | 1.757 | 1.826 | 4.798 | 4.629 | 4.970 | 5.885 | 5.849 | 5.798 | 9.232 | 9.281 | 2.750 | 2.742 |
| Ca | 0.905 | 0.844 | 0.003 | 0.010 | 0.000 | 0.000 | 0.003 | 0.003 | 1.919 | 1.998 | 0.000 | 0.005 | 0.003 | 0.004 | 0.012 | 0.004 | 0.001 | 0.000 |
| Na | 0.023 | 0.058 | 0.000 | 0.000 | 0.000 | 0.000 | 0.001 | 0.000 | 0.018 | 0.014 | 0.002 | 0.007 | 0.115 | 0.077 | 0.015 | 0.015 | 0.000 | 0.000 |
| K | 0.000 | 0.001 | 0.000 | 0.000 | 0.000 | 0.000 | 0.000 | 0.000 | 0.003 | 0.003 | 0.005 | 0.004 | 0.002 | 0.002 | 0.015 | 0.005 | 0.000 | 0.000 |
| Ni | 0.000 | 0.002 | 0.000 | 0.041 | 0.000 | 0.000 | 0.000 | 0.001 | — | — | — | — | — | — | — | — | 0.000 | 0.000 |
| Sum | 4.000 | 3.999 | 24.008 | 24.000 | 3.001 | 3.001 | 4.000 | 4.000 | 14.941 | 15.015 | 13.007 | 13.016 | 14.001 | 14.001 | 19.903 | 19.975 | 4.937 | 4.928 |

Table 2

Geochemical compositions of Jandaq (upper, samples J) and Ashin (lower, samples A) ophiolite mantle peridotites (central Iran) (Major elements in wt.%, trace elements in ppm, and *: ppb). Lz: herzolite, Hz: harzburgite, Du: dunite.

Tableau 2

Compositions chimiques des péridotites mantelliques des ophiolites de Jandaq (en haut, échantillons J) et Ashin (en bas, échantillons A). (Éléments majeurs en pds%, trace en ppm, * : ppb). Lz : herzolite, Hz : harzburgite, Du : dunite.

| Sample | SiO ₂ | TiO ₂ | Al ₂ O ₃ | Cr ₂ O ₃ | Fe ₂ O ₃ * | MnO | MgO | CaO | Na ₂ O | K ₂ O | NiO | LOI | Co | Sc | V | La | Sm | Dy | Yb |
|-------------|------------------|------------------|--------------------------------|--------------------------------|----------------------------------|-------------|--------------|-------------|-------------------|------------------|-------------|--------------|------------|-----------|-----------|-------------|-------------|-------------|-------------|
| J685 (Lz) | 44.18 | 0.08 | 1.19 | 0.10 | 6.25 | 0.12 | 33.68 | 5.41 | 0.03 | 0.01 | 0.12 | 9.05 | 47 | 4 | 14 | 0.31 | 0.33 | 2.33 | 0.33 |
| J688 (Lz) | 39.70 | 0.23 | 3.91 | 0.31 | 13.5 | 0.17 | 33.32 | 2.01 | 0.04 | 0.01 | 0.29 | 7.10 | 77 | 5 | 86 | 4.80 | 2.29 | 2.67 | 2.47 |
| J715 (Lz) | 39.88 | 0.13 | 3.55 | 0.50 | 12.07 | 0.15 | 35.79 | 1.26 | 0.22 | 0.01 | 0.18 | 6.94 | 97 | 17 | 59 | 0.22 | 0.15 | 1.24 | 0.31 |
| J716 (Lz) | 42.99 | 0.12 | 4.14 | 0.66 | 8.14 | 0.09 | 26.59 | 11.32 | 0.07 | 0.01 | 0.25 | 6.53 | 56 | 36 | 123 | 0.28 | 0.30 | 1.85 | 0.52 |
| J718 (Lz) | 41.36 | 0.13 | 5.65 | 0.42 | 11.25 | 0.13 | 29.34 | 5.57 | 0.03 | 0.01 | 0.14 | 6.52 | 73 | 18 | 60 | 0.95 | 0.22 | 1.53 | 0.40 |
| J719 (Lz) | 39.81 | 0.23 | 5.95 | 0.42 | 9.06 | 0.10 | 27.54 | 10.47 | 0.11 | 0.02 | 0.17 | 6.71 | 72 | 29 | 96 | 0.28 | 0.33 | 2.07 | 0.46 |
| J720 (Lz) | 41.44 | 0.12 | 3.61 | 0.34 | 10.71 | 0.11 | 33.11 | 2.95 | 0.03 | 0.01 | 0.20 | 7.92 | 96 | 14 | 38 | 0.19 | 0.11 | 2.11 | 0.37 |
| J721 (Lz) | 39.58 | 0.15 | 8.07 | 0.03 | 7.82 | 0.09 | 29.97 | 7.39 | 0.05 | 0.01 | 0.14 | 6.86 | 71 | 16 | 52 | 0.23 | 0.14 | 2.00 | 0.37 |
| J722 (Lz) | 41.42 | 0.13 | 5.48 | 0.35 | 8.94 | 0.11 | 32.38 | 4.32 | 0.06 | 0.01 | 0.15 | 7.14 | 85 | 20 | 62 | 0.35 | 0.17 | 2.01 | 0.38 |
| J723 (Lz) | 41.67 | 0.18 | 4.08 | 0.72 | 7.35 | 0.11 | 25.47 | 12.33 | 0.13 | 0.02 | 0.27 | 8.66 | 91 | 47 | 149 | 0.43 | 0.45 | 2.00 | 0.86 |
| J724 (Lz) | 44.77 | 0.23 | 4.57 | 0.75 | 7.25 | 0.11 | 23.48 | 12.45 | 0.15 | 0.02 | 0.01 | 6.97 | 78 | 48 | 150 | 0.34 | 0.46 | 2.37 | 0.63 |
| J725 (Lz) | 43.32 | 0.13 | 5.82 | 0.22 | 9.58 | 0.11 | 30.49 | 3.74 | 0.04 | 0.01 | 0.22 | 6.77 | 86 | 13 | 44 | 0.21 | 0.13 | 2.25 | 0.42 |
| J728 (Lz) | 43.16 | 0.08 | 0.79 | 0.48 | 8.22 | 0.11 | 37.95 | 0.70 | 0.04 | 0.01 | 0.27 | 8.93 | 71 | 7 | 31 | 0.15 | 0.10 | 2.34 | 0.29 |
| J729 (Lz) | 44.22 | 0.09 | 0.89 | 0.39 | 7.75 | 0.13 | 35.83 | 0.78 | 0.04 | 0.02 | 0.34 | 10.26 | 118 | 7 | 33 | 0.19 | 0.12 | 2.10 | 0.34 |
| J731 (Lz) | 42.83 | 0.07 | 0.85 | 0.50 | 8.38 | 0.07 | 36.97 | 0.91 | 0.04 | 0.01 | 0.29 | 9.87 | 74 | 12 | 34 | 0.18 | 0.13 | 1.81 | 0.37 |
| J732 (Lz) | 44.93 | 0.06 | 1.15 | 0.51 | 7.79 | 0.08 | 36.14 | 0.70 | 0.04 | 0.01 | 0.42 | 9.10 | 99 | 10 | 42 | 0.16 | 0.11 | 1.91 | 0.32 |
| J740 (Lz) | 43.93 | 0.08 | 0.98 | 0.31 | 6.73 | 0.05 | 37.88 | 0.98 | 0.04 | 0.01 | 0.31 | 9.32 | 77 | 7 | 18 | 0.19 | 0.12 | 1.21 | 0.51 |
| J741 (Lz) | 44.46 | 0.08 | 1.36 | 0.34 | 7.25 | 0.09 | 32.40 | 5.04 | 0.20 | 0.16 | 0.23 | 8.96 | 66 | 7 | 35 | 1.14 | 0.11 | 2.24 | 0.58 |
| J748 (Lz) | 40.52 | 0.15 | 2.95 | 0.75 | 13.01 | 0.13 | 34.40 | 0.70 | 0.02 | 0.01 | 0.24 | 8.12 | 94 | 11 | 67 | 0.16 | 0.11 | 2.31 | 0.37 |
| J772 (Lz) | 43.76 | 0.08 | 0.66 | 0.39 | 7.06 | 0.07 | 37.47 | 0.98 | 0.04 | 0.01 | 0.32 | 9.87 | 83 | 7 | 33 | 0.22 | 0.14 | 1.79 | 0.33 |
| J773 (Lz) | 40.79 | 0.22 | 2.72 | 0.38 | 9.44 | 0.10 | 36.44 | 0.98 | 0.03 | 0.01 | 0.34 | 9.28 | 77 | 9 | 62 | 1.84 | 0.75 | 2.09 | 1.15 |
| J622 (Hz) | 43.62 | 0.10 | 1.29 | 0.35 | 5.45 | 0.08 | 38.96 | 0.84 | 0.02 | 0.01 | 0.31 | 9.64 | 77 | 7 | 37 | 0.12 | 0.10 | 1.67 | 0.36 |
| J762 (Hz) | 43.75 | 0.20 | 2.10 | 0.04 | 7.55 | 0.08 | 35.35 | 0.77 | 0.68 | 0.01 | 0.20 | 9.52 | 67 | 10 | 43 | 0.41 | 0.18 | 1.70 | 0.42 |
| J769 (Hz) | 37.20 | 0.08 | 3.70 | 0.10 | 10.14 | 0.11 | 40.47 | 0.84 | 0.02 | 0.01 | 0.19 | 7.43 | 89 | 8 | 26 | 0.25 | 0.15 | 1.99 | 0.34 |
| J770 (Hz) | 38.64 | 0.12 | 3.91 | 0.03 | 11.18 | 0.13 | 36.94 | 0.91 | 0.02 | 0.01 | 0.17 | 8.15 | 92 | 12 | 35 | 0.20 | 0.12 | 2.02 | 0.32 |
| Mean | 42.08 | 0.13 | 3.17 | 0.38 | 8.87 | 0.11 | 33.53 | 3.77 | 0.09 | 0.02 | 0.23 | 8.22 | 80 | 15 | 57 | 0.55 | 0.29 | 1.98 | 0.53 |
| A50 (Lz) | 42.61 | 0.10 | 2.06 | 0.42 | 8.19 | 0.13 | 36.03 | 1.58 | 0.03 | 0.01 | 0.25 | 8.58 | 140 | 14 | 68 | <0.08 | <0.10 | <0.45 | <0.14 |
| A201 (Lz) | 34.46 | 0.08 | 2.72 | 0.38 | 8.28 | 0.13 | 39.09 | 2.57 | 0.06 | 0.01 | 0.25 | 11.96 | 92 | 14 | 80 | <0.05 | <0.10 | <0.30 | 0.25 |
| A222 (Lz) | 36.10 | 0.08 | 2.97 | 0.35 | 8.72 | 0.12 | 40.02 | 2.92 | 0.13 | 0.01 | 0.24 | 8.33 | 98 | 14 | 83 | <0.07 | <0.12 | <0.30 | <0.10 |
| A249 (Lz) | 37.68 | 0.06 | 1.49 | 0.45 | 7.72 | 0.12 | 40.19 | 1.87 | 0.03 | 0.01 | 0.22 | 10.15 | 90 | 12 | 64 | 48* | <0.10 | <0.30 | <0.08 |
| A287 (Lz) | 38.82 | 0.06 | 1.23 | 0.34 | 7.71 | 0.11 | 37.63 | 0.95 | 0.03 | 0.02 | 0.24 | 12.86 | 100 | 11 | 47 | <0.08 | <0.11 | <0.30 | <0.12 |
| A322 (Lz) | 41.89 | 0.09 | 1.34 | 0.44 | 9.49 | 0.13 | 30.87 | 6.46 | 0.06 | 0.01 | 0.11 | 9.10 | 95 | 32 | 98 | <0.07 | 0.12 | <0.40 | <0.35 |
| A424 (Lz) | 37.58 | 0.06 | 1.17 | 0.41 | 7.72 | 0.11 | 37.53 | 1.34 | 0.03 | 0.01 | 0.29 | 13.74 | 105 | 10 | 46 | <0.06 | <0.10 | <0.36 | <0.10 |
| A425 (Lz) | 40.37 | 0.07 | 3.06 | 0.42 | 8.21 | 0.12 | 35.98 | 2.52 | 0.09 | 0.02 | 0.28 | 8.86 | 100 | 13 | 72 | <0.08 | 0.23 | <0.40 | 0.33 |
| A468 (Lz) | 37.21 | 0.06 | 1.23 | 0.42 | 7.43 | 0.11 | 38.93 | 1.43 | 0.02 | 0.01 | 0.29 | 12.86 | 101 | 10 | 49 | <0.06 | <0.09 | <0.30 | <0.10 |
| A473 (Lz) | 41.29 | 0.07 | 2.82 | 0.38 | 7.72 | 0.11 | 34.87 | 2.84 | 0.13 | 0.02 | 0.31 | 9.45 | 97 | 13 | 75 | <0.08 | 0.14 | 0.27 | 0.44 |
| A399 (Hz) | 39.04 | 0.05 | 0.81 | 0.37 | 7.56 | 0.08 | 38.41 | 0.36 | 0.03 | 0.01 | 0.31 | 12.97 | 104 | 6 | 28 | 62* | <0.08 | <0.26 | <0.50 |
| A400 (Hz) | 38.15 | 0.06 | 1.06 | 0.58 | 7.53 | 0.07 | 38.66 | 0.53 | 0.02 | 0.00 | 0.32 | 13.01 | 108 | 8 | 43 | <0.10 | <0.09 | <0.27 | <0.10 |
| A419 (Hz) | 37.67 | 0.07 | 1.97 | 0.51 | 8.62 | 0.11 | 36.61 | 0.36 | 0.02 | 0.01 | 0.32 | 13.73 | 120 | 14 | 83 | <0.08 | <0.09 | <0.36 | <0.12 |
| A476 (Hz) | 38.36 | 0.06 | 0.76 | 0.37 | 6.95 | 0.11 | 39.31 | 0.31 | 0.02 | 0.01 | 0.33 | 13.42 | 96 | 8 | 37 | <0.07 | <0.10 | <0.30 | <0.10 |
| A504 (Hz) | 38.61 | 0.06 | 1.36 | 0.47 | 6.98 | 0.11 | 36.66 | 1.75 | 0.03 | 0.02 | 0.28 | 13.68 | 93 | 11 | 53 | <0.06 | <0.11 | 0.29 | <0.10 |
| A514 (Hz) | 37.21 | 0.06 | 1.21 | 0.29 | 6.58 | 0.08 | 40.34 | 0.34 | 0.02 | 0.01 | 0.29 | 13.58 | 94 | 10 | 45 | <0.06 | <0.11 | <0.32 | <0.10 |
| A503 (Du) | 38.43 | 0.07 | 1.98 | 0.70 | 7.35 | 0.13 | 36.95 | 0.32 | 0.11 | 0.01 | 0.32 | 13.62 | 107 | 21 | 90 | <0.09 | <0.10 | <0.32 | <0.14 |
| A505 (Du) | 33.51 | 0.07 | 1.42 | 0.47 | 10.08 | 0.18 | 39.49 | 1.12 | 0.03 | 0.01 | 0.22 | 13.41 | 119 | 9 | 40 | 50* | <0.09 | <0.35 | <0.10 |
| A506 (Du) | 33.85 | 0.06 | 0.70 | 0.92 | 8.66 | 0.14 | 37.83 | 0.48 | 0.02 | 0.01 | 0.28 | 17.05 | 117 | 7 | 36 | <0.06 | <0.10 | <0.35 | <0.10 |
| Mean | 38.04 | 0.07 | 1.65 | 0.46 | 7.97 | 0.12 | 37.65 | 1.58 | 0.05 | 0.01 | 0.27 | 12.12 | 104 | 12 | 60 | — | — | — | — |

less abundant than tremolite. Anthophyllite can be recognized by its parallel extinction and lack of twinning. This mineral makes sheaf-like aggregates (Fig. 3F). Concentrations of MgO ranges from 33 to

34.16 wt.%, and abundance of Na₂O is very low (< 0.03 wt.%). This orthoamphibole has a restricted stability field between approximately 600 and 800 °C at pressures below 12 kbar [29].

- Chlorite (peninite with Mg# 0.90–0.91) is present with faintly green pleochroic in matrix and sometimes in veinlets of studied rocks. Presence of this mineral is another evidence of the last retrograde metamorphism in greenschist facies. Cr₂O₃ content of analyzed chlorites is 0.08 to 0.30 wt.%.
- Antigorite (Mg# 0.89–0.98), which is colorless or less commonly pale green, is dominant constituent of Jandaq ophiolite metamorphosed mantle peridotites. It occurs mostly as fine-grained crystals. Antigorite has partially replaced and surrounded the metamorphic olivines by the last metamorphic episode. This mineral identified by microprobe analyses and XRD pattern. Antigorites have a wide range of Mg# (0.89–0.98) and Al₂O₃ contents (1.35–4.12 wt.%). The upper stability limit of antigorite is between 500 and 600 °C [31].
- Talc (Mg# 0.98) is common in orthopyroxene bearing rock samples. It is not aligned with respect to a foliation. The Na₂O and Al₂O₃ contents of analyzed talcs range from 0.11–0.46 and 0.45–2.12 wt.%, respectively.

Based on the petrography and mineral assemblages, two rock types are distinguished in mantle peridotite section of Jandaq ophiolite:

- (1) Metalherzolites (clinopyroxene + spinel + olivine + tremolite + chlorite + serpentine + magnetite ± calcite);
- (2) Metaharzburgites (olivine + orthopyroxene + talc + anthophyllite + magnetite + spinel ± low amounts of chlorite and tremolite).

4. Whole rock chemistry

Table 2 lists the chemical compositions of 44 whole rock samples. Twenty-five samples from mantle peridotites of the Jandaq ophiolite and 19 samples from the Ashin ophiolite analysed to find the chemical nature of studied ultramafic system. The mean of analyzed samples from each ophiolite is presented in lower row.

All the analyzed samples from the Jandaq ophiolite are rich in MgO (23.48–40.47 wt.%), with wide range in the concentrations of Fe₂O₃* (5.45–13.5 wt.%), Al₂O₃ (0.66–8.07 wt.%) and CaO (0.70–12.45 wt.%). Cr₂O₃ and TiO₂ contents are 0.04–0.75 wt.% and 0.06–0.23 wt.%, respectively. Considerable amounts of LOI confirm the extensively serpentinization of these rocks and presence of hydrous minerals. The lherzolite samples which contain considerable amount of relict

clinopyroxene (J716, J719, J723 and J724), present the highest contents of CaO, Sc and V. Low-CaO lherzolites are essentially made by serpentine and fine-grained tremolite.

Study of whole rocks chemical composition shows similarity of all analyzed rock samples with the pattern of mantle peridotites from ocean basins. Comparison of whole rocks chemical composition from the Jandaq and Ashin ophiolites and using the mean of analyses reveals that the Jandaq ophiolite samples have lower contents of MgO, Cr₂O₃, MnO, NiO, Co, V and higher amounts of SiO₂, TiO₂, Al₂O₃, Fe₂O₃*, CaO, Na₂O, K₂O, Sc and REE. These chemical characteristics show the undepleted nature of mantle peridotites in Jandaq ophiolite.

5. Discussion

5.1. Metamorphic condition of P-T equilibration

The dominant metamorphic mineralogy of these rocks included olivine, tremolite, orthopyroxene, talc, anthophyllite, chlorite, serpentine and magnetite. Based on the mineralogical composition and using the scheme of Evans [14], these mineral assemblages correspond to tremolite peridotite, which is indicative of the amphibolite facies that followed by green schist facies. These results are confirmed by Table 13- 2 in Spear [28], mineralogical study of amphibolites, and using the amphibole barometry and amphibole-plagioclase thermometry [33]. Subsequent amphibolite to greenschist facies retrogression modified the mineralogy of these progressively metamorphosed mantle peridotites, as evidenced especially by serpentinization of metamorphic olivines and orthopyroxenes, late growth of chlorite and thin veins of serpentine developed in the ultramafic rocks.

5.2. Petrogenesis

The fertile lherzolite in the mantle section of the Jandaq ophiolite is a predominant rock unit based on the field and the petrographical studies. Abundance of lherzolite, low amount of harzburgite and dunite, and limited amount of amphibolite (formerly basic volcanic rocks) in this ophiolite reveals that the partial melting and continual melt production is not an extensive phenomenon in this mantle section. Therefore, the volume of ascending melt should be low and wall rock/melt interactions would not occur in large scale. According to the quantitative melting indicator for mantle residues [16] and using the composition of spinels from the Jandaq ophiolite, the degree of partial

melting is lower than 18%. But the field investigations, small harzburgite layers which are uniformly dispersed within the lherzolite and considering the very high lherzolite/harzburgite ratio, show that these partial meltings are discrete and non-pervasive episodes in this ophiolite.

Highly variable contents of Al_2O_3 in analyzed samples (0.79–8.07 wt.%) is one of characteristics of orogenic lherzolites [9]. Low amounts of Cr_2O_3 associated with highly variable content in Al_2O_3 appear as characteristics of peridotite massifs [9], compared to cratonic and abyssal peridotites that show a large spread of Cr_2O_3 whole rock content correlated with Al_2O_3 content. The contents of other mildly incompatible elements as V, Sc and Yb, in whole rock chemical data of Jandaq mantle peridotites, and Cr_2O_3 content of clinopyroxenes, support this idea. It resembles that the Jandaq mantle peridotites provide us the Earth's mantle with unique exposure. Mineral chemistry of clinopyroxenes (diopsides) reveals the sub-oceanic crust mantle origin of the Jandaq peridotites (Fig. 4A and B).

Several recent contributions (e.g. [7,20,21]) suggest that a number of lherzolites could represent refertilized mantle, that is depleted (harzburgitic) mantle in which percolating magma crystallized secondary clinopyroxene. In this case, the Cr_2O_3 content of clinopyroxene is not marker of the initial fertility of the peridotite concerning this element. However, in the case of Jandaq ophiolite, field studies, transitional succession of lherzolite – harzburgite – dunite, absence of lherzolite – dunite contact, homogeneous rock samples in mineralogy, and low degree of partial melting, reject

this hypothesis. Using Le Roux [21], whole rock versus mineral chemistry discriminant diagram, supports partial melting trend instead of refertilization one.

About of using the chemical composition of whole rocks and minerals, in Paleo-tectonic reconstruction of ophiolites, Nicolas and Boudier [25] discuss the validity of geochemical discrimination diagrams in their application to ophiolite environments. In particular, they question the validity of Cr# in spinel by reference to abyssal peridotite data [2,12]. They reveal that the common used discriminant diagrams do not discriminate anything. Therefore, the geotectonic discrimination diagrams are not used in this article.

5.3. Characterization of the ophiolite type

According to the petrography and considering the clinopyroxene relict and tremolite modal contents, it can be concluded that the protolith of poly-metamorphosed mantle peridotites of the Jandaq ophiolite have originally been lherzolite (most) and harzburgite (less), and dunites are rare in this ophiolite. This points to LOT characteristic of this ophiolite, but anyway, it should be noted that the distinction between LOT and HOT ophiolites is not straightforward by petrography of poly-metamorphosed mantle peridotites and more evidences are needed (e.g. whole rock chemical data).

Considerable amounts of TiO_2 , Al_2O_3 , CaO , Na_2O , K_2O , Sc and REE in the Jandaq samples, points to LOT nature of the Jandaq mantle peridotites and supports the petrographical results. By wide spread partial melting

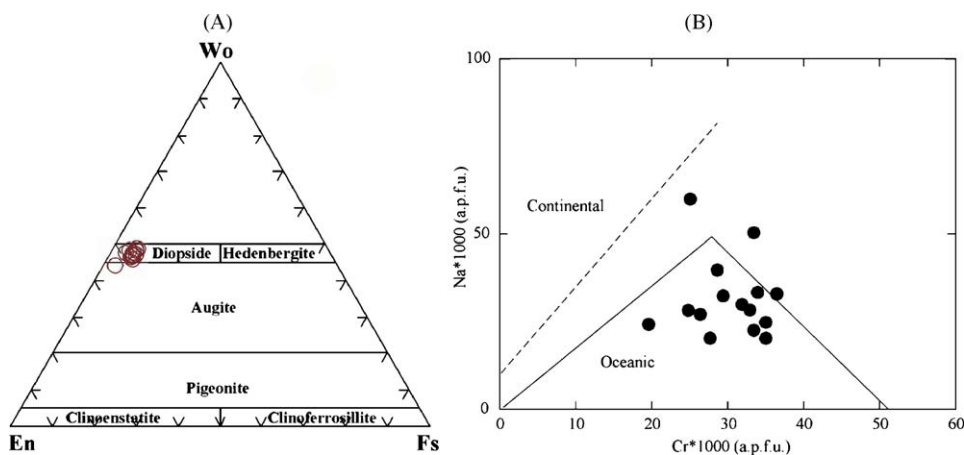


Fig. 4. Chemical diagrams of clinopyroxenes. (A) Ternary of pyroxenes classification and diopside composition of Jandaq clinopyroxenes, (B) Atomic Cr and Na content of clinopyroxenes formula unit to confirm oceanic nature of the Jandaq peridotites. The diagram is from [17].

Fig. 4. Diagrammes chimiques des clinopyroxènes. (A) Classification ternaire des pyroxènes, indiquant la composition diopsidique des clinopyroxènes de Jandaq, (B) Pourcentage atomique Cr et Na dans la formule-unité des clinopyroxènes, confirmant la nature océanique des péridotites de Jandaq. Le diagramme provient de [17].

and continual basaltic melt production, the contents of these elements will decrease. Presence of lherzolites with high content of CaO (10.47–12.45 wt.%), and considerable amount of modal clinopyroxene (ranges up to 30%), can be interpreted as intact peridotites of mantle. Alternately, the low TiO₂, Al₂O₃, CaO, Na₂O, K₂O, Sc and REE contents in the Ashin ophiolite mantle peridotites argue for the HOT nature of this ophiolite, high degree of pervasive and continual partial melting and clinopyroxene removal for production of primary basaltic melt.

5.4. Implications for chromitite potential

The above two sections (5.2 and 5.3) reveal that the Jandaq ophiolite is characterized by a lherzolitic mantle section and belongs to the Lherzolite Ophiolite Type (LOT). Therefore, based on the general rule, the chromitite should be generally absent. Arai [4] shows that in Al-rich mantle peridotites (as Jandaq ophiolite that amount of Al₂O₃ reaches up to 8.07 wt.%), the podiform chromitite is almost absent or very small in amount.

Comparison of chemical whole rock data from the Jandaq (as a LOT) and Ashin ophiolites (as a HOT) reveals that the Cr₂O₃ content of mantle peridotites from the Ashin ophiolite (0.46 wt.%) is higher than that in the Jandaq ophiolite (0.38 wt.%), in spite of abundant chromitite formation in the Ashin ophiolite. This difference shows that the Cr₂O₃ content of the Jandaq ophiolite originally was low and this mantle is not suitable for considerable chromitite formation through high degree of partial melting and wide spread melt-wall rock reaction.

The study of chemical composition of clinopyroxenes shows that the chromium hosted by pyroxenes, is still largely retained by these mineral and may form limited chromitite after high degree of partial melting. The range of Cr₂O₃ content in clinopyroxenes is 0.71–1.31 wt %.

6. Conclusions

In Jandaq meta-ophiolite, the predominant mantle peridotite is lherzolite, which composed of clinopyroxene, spinel, olivine, tremolite, chlorite, serpentine and magnetite. Geochemically, the minerals and whole rock samples appear as orogenic peridotite massifs. The main geochemical characteristics of these fertile peridotites are low amount of Cr₂O₃ and highly variable content of Al₂O₃. Based on the field and petrographical studies, chemistry of minerals and whole rock samples,

the Jandaq peridotites belong to the LOT (Lherzolite Ophiolite Type), and have no chromite concentration potentiality, following the thermal structure and chemical composition.

Acknowledgment

The author is indebted to Professor Adolphe Nicolas, Professor Jacques Léon Robert Touret and Professor Françoise Boudier for providing useful comments on the manuscript. Supports of the University of Isfahan, Dr. Jurgen Koepke and Leibniz University are gratefully acknowledged.

References

- [1] M. Alavi, Tectonic Map of the Middle East, Geological Survey of Iran, Scale: 1:5,000,000, 1991.
- [2] J.F. Allan, H.J.B. Dick, Proceedings of the ocean drilling program, scientific results 1467 (1996) 157–172.
- [3] M. Almasian, Tectonics of the Anarak area (central Iran), PhD thesis (Unpublished), Islamic Azad University, Science and Research Unit, Iran, 1997, 164 p.
- [4] S. Arai, Control of Wall-rock composition on the formation of Podiform Chromitites as a result of Magma/Peridotite Interaction, *Resour. Geol.* 47 (4) (1997) 177–187.
- [5] S. Arai, Origin of podiform chromitites, *J. Asian Earth Sci.* 15 (1997) 303–310.
- [6] S. Bagheri, The exotic Paleo-Tethys terrane in central Iran: new geological data from Anarak, Jandaq and Posht-e-Badam areas, PhD thesis, Faculty of Geosciences and Environment, University of Lausanne, Switzerland, 2007, 208 p.
- [7] J.L. Bodinier, M. Godard, Orogenic, ophiolitic, and abyssal peridotites, in : R.W. Carlson (Ed.), *Treatise on Geochemistry*, Elsevier Science Ltd, 2003, pp. 103–170.
- [8] F. Boudier, A. Nicolas, Harzburgite and lherzolite subtypes in ophiolitic and oceanic environments, *Earth Planet. Sci. Lett.* 76 (1–2) (1985) 84–92.
- [9] D. Canil, Mildly incompatible elements in peridotite and the origins of mantle lithosphere, *Lithos* 77 (2004) 375–393.
- [10] M. Davoudzadeh, Geology of Iran, in : E.M. Moores, R.W. Fairbridge (Eds.), *Encyclopedia of Asian and European Regional Geology*, Chapman & Hall, London, 1997, pp. 384–405.
- [11] M. Davoudzadeh, G. Lensch, K.W. Diefenbach, Contribution to the paleogeography, stratigraphy and tectonics of the Infracambrian and Lower Paleozoic of Iran, *N. Jb. Geol. Paläont. Abh.* 172 (1986) 245–269.
- [12] H.J.B. Dick, T. Bullen, Chromian spinel as a petrogenetic indicator in abyssal and alpine-type peridotites and spatially associated lavas, *Contrib. Mineral. Petrol.* 86 (1984) 54–76.
- [13] G.T.R. Droop, A general equation for estimating Fe³⁺ concentrations in ferromagnesian silicates and oxides from microprobe analyses, using stoichiometric criteria, *Mineral. Mag.* 51 (1987) 431–435.
- [14] B.W. Evans, Metamorphism of Alpine peridotite and serpentine, *Ann. Rev. Earth Planet. Sci.* 5 (1977) 397–445.
- [15] F. Gervilla, M. Leblanc, Magmatic ores in high-temperature Alpine-type lherzolite massifs Ronda Spain, and Beni. Bousera, Morocco, *Econ. Geol.* 85 (1990) 112–132.

- [16] E. Hellebrand, J.E. Snow, H.J.B. Dick, A.W. Hofmann, Coupled major and trace elements as indicators of the extent of melting in mid-ocean-ridge peridotites, *Nature* 410 (2001) 677–681.
- [17] J. Kornprobst, D. Ohnenstetter, M. Ohnenstetter, Na and Cr contents in Cpx from peridotites: a possible discriminant between sub-continental and sub-oceanic mantle, *Earth Planet. Sci. Lett.* 53 (1981) 241–254.
- [18] R. Kretz, Symbols for rock-forming minerals, *Am. Mineral.* 68 (1983) 277–279.
- [19] B.L. Lago, M. Rabinowicz, A. Nicolas, Podiform chromite ore bodies: A genetic model, *J. Petrol.* 23 (1982) 103–125.
- [20] X. Lenoir, C.J. Garrido, J.L. Bodinier, J.M. Dautria, F. Gervilla, The recrystallization front of the Ronda peridotite: evidence for melting and thermal erosion of subcontinental lithospheric mantle beneath the Alboran Basin, *J. Petrol.* 42 (1) (2001) 141–158.
- [21] V. Le Roux, J.L. Bodinier, A. Tommasi, O. Alard, J.M. Dautria, A. Vauchez, A.J.V. Riche, The Lherz spinel lherzolite: Refertilized rather than pristine mantle, *Earth Planet. Sci. Lett.* 259 (3–4) (2007) 599–612.
- [22] S.J. Lippard, A.W. Shelton, I.G. Gass, The ophiolites of northern Oman, *Geol. Soc. Lond. Mem.* 11 (1986) 178.
- [23] A. Nicolas, Structures of ophiolites and dynamics of oceanic lithosphere, Dordrecht, Kluwer Academic Publishers, Netherlands, 1989, 367 p.
- [24] A. Nicolas, H. Al Azri, in : Proceedings of the ophiolite conference, held in Muscat, Oman, Chromite-rich and chromite-poor ophiolites: the Oman case, (1990), pp. 261–274.
- [25] A. Nicolas, F. Boudier, Where ophiolites come from and what they tell us, *Geol. Soc. Spec. Pap.* 373 (2003) 137–152.
- [26] A.D. Paktunc, Metamorphism of the ultramafic rocks of the Thompson Mine, Thompson Nickel Belt, Northern Manitoba, *Can. Mineral.* 22 (1984) 77–91.
- [27] S. Roberts, Ophiolitic chromitite formation: a marginal basin phenomenon? *Econ. Geol.* 83 (1988) 1034–1036.
- [28] E. Romanko, Yu Kokorin, B. Krivyakin, M. Susov, L. Morozov, M. Sharkovski, Outline of metallogeny of Anarak area (Central Iran), Geological Survey of Iran, V/O “Technoexport”, Report TE/No. 21, 1984, 136 p.
- [29] F.S. Spear, Metamorphic phase equilibria and pressure-temperature-time paths, Mineralogical Society of America, 1995, 799 p.
- [30] G. Torabi, Petrology of Anarak area ophiolites (central Iran, NE of Isfahan Province), PhD thesis in petrology (Unpublished), Tarbiat Modarres University, Iran, 2003, 249 p.
- [31] G. Torabi, Detection of pressure and temperature in formation of Jandaq ophiolite amphibolites (NE of Isfahan province, Iran) by using amphibole and plagioclase barometry and thermometry, *J. Iran. Soc. Cryst. Mineral.* 15 (1) (2007) 117–134.
- [32] A. Yaghubpur, A.A. Hassannejad, The spatial distribution of some chromite deposits in Iran, using fry analysis, *J. Sci. Islam. Rep. Iran* 17 (2) (2006) 147–152.
- [33] Yumul G.P.Jr., The Cretaceous Southeast Bohol ophiolite complex, central Philippines: evidence for formation in a fast spreading center, *J. Asian Earth Sci.* 21 (2003) 957–965.
- [34] F.M. Zhou, P.T. Robinson, W.J. Bai, Formation of podiform chromitites by melt/rock interaction in the upper mantle, *Miner. Deposita* 29 (1994) 98–101.